

# Performance Evaluation of a Neural Network Model and Two Empirical Models for Estimating Soil Moisture Based on Sentinel-1 SAR Data

Yan Li<sup>1</sup>, Songhua Yan<sup>2, 3, \*</sup>, Nengcheng Chen<sup>4</sup>, and Jianya Gong<sup>2, 3</sup>

**Abstract**—The objective of this paper is to propose an inversion model of soil moisture using a neural network and compare the performance of this method with two empirical models in soil moisture inversion. A wide dataset of backscattering coefficients extracted from Sentinel-1 images and in-situ soil surface parameter measurements (moisture content and roughness) are used. Since the available backscattering models have limited performances of describing the nonlinear relationship between soil parameters and backscatter coefficient, the retrieval of soil parameters from radar backscattering coefficient remains challenging. The proposed inversion method of a neural network is used for establishing this relationship. At the same time, two empirical models are employed to estimate the soil moisture for comparison. The results show that for most of the six measuring stations the inverted soil moisture with the neural network model has higher correlation coefficient with the in-situ soil moisture than those by the empirical models. Moreover, the neural network model inversion results under multi-polarization input conditions are discussed in this paper. The results of stations 2, 4, and 5 show that  $R^2$  of multi-polarization inputs are increased by 0.1928, 0.4821, and 0.2758, respectively, compared with those of single-polarization inputs.

## 1. INTRODUCTION

Surface soil moisture is one of the important variables, helping to understand the physical process between the land and the atmosphere. Thus, the temporal and spatial distribution of soil moisture is crucial for a sustainable environment. For example, crop growth and development can be analyzed by collecting soil moisture datasets timely. Hence, soil moisture monitoring is necessary for agricultural development [1–5]. Two methods are commonly used for monitoring, namely optical remote sensing and microwave remote sensing. However, optical remote sensing images are easily obscured by clouds due to the short wavelength. Therefore, synthetic aperture radar (SAR) satellite remote sensing based on microwave scattering becomes an important method for long-term soil parameters monitoring over large areas [6–8].

The use of SAR data to monitor soil moisture has been demonstrated in numerous studies. Some empirical or semi-empirical models for soil moisture inversions were proposed, such as Dubois model [9], IEM [10], and Oh models [11, 12]. At present, these models are still widely used in the study of various soil moisture. However, empirical models have some limitations [13, 14]. For example, due to different surface roughness caused by topography, the inversion results sometimes show poor correlation. Therefore, Baghdadi et al. [15] proposed a modified Dubois model, whose results prove that the simulated backscattering coefficients acquired from the modified model are closer to SAR data than that from the

---

*Received 16 July 2020, Accepted 28 August 2020, Scheduled 8 September 2020*

\* Corresponding author: Songhua Yan (ysh@whu.edu.cn).

<sup>1</sup> School of Electronic Information, Wuhan University, Wuhan, China. <sup>2</sup> School of Remote Sensing and Information Engineering, Wuhan University, Wuhan, China. <sup>3</sup> Institute of Aerospace Science and Technology, Wuhan University, Wuhan, China. <sup>4</sup> State Key Laboratory of Information Engineering in Surveying, Mapping and Remote Sensing, Wuhan University, Wuhan, China.

original one. Also, since empirical models consider soil parameters (roughness and moisture) and the incidence angle in the inversion of soil moisture, Sekertekin et al. [16] used multiple linear regression (MLR) analysis to associate these three variables mentioned above, and hence established a developed empirical model. Nevertheless, there has been no literature on the comparison of the performances of MLR analysis and the modified Dubois model in soil water inversion. A new attempt in our study is a comparative study of the capability of c-band radar inversion in the MLR analysis and the modified Dubois model.

Moreover, neural networks have become a hot topic in various fields in recent years. A complex mapping relationship between radar backscatter coefficient and soil moisture exists, and the quantitative relationship is unclear. Therefore, a neural network is used to establish the relationship in our paper. Neural networks have a good performance in both fitting and prediction. Several studies use the combination of neural networks and empirical models to map soil moisture [17–19]. Mirsoleimani et al. [20] proposed to simulate backscattering dataset with IEM and WCM models to train neural networks, and then used the Sentinel-1 data to retrieve moisture. Although using the dataset simulated by the empirical model and combining with a neural network can meet the demand of water inversion, the problem of inconsistency exists between the simulated dataset and measured dataset. As a result, the neural network is accurate to the theoretical value and inaccurate to the measured value. These retrieval approaches are therefore unsuitable for the field environment in many areas.

The aim of this study is to investigate the ability of the modified Dubois model, MLR analysis, and a neural network model in soil moisture inversion using measured datasets. Several experiments have investigated that both  $VV$  and  $VH$  polarization backscatter coefficients have an excellent performance in the inversion of soil moisture [21, 22]. Therefore,  $VV$  polarization data of Sentinel-1 in the Baoxie area of Wuhan are selected as an example in this study. From November 2019 to April 2020, 12 SAR images were selected, and field data from 6 measurement sites were analyzed. By training and testing the data using three inversion methods,  $R^2$  and RMSE between the estimated moisture and the in-situ moisture are calculated. The results show that the neural network provides soil moisture estimation with high accuracy.

This paper is organized as follows. Section 2 describes the relationship between the radar backscattering coefficient and soil parameters. Section 3 presents two empirical models for soil moisture. Section 4 provides the neural network used for retrieving soil moisture. Section 5 presents the acquisitions of datasets such as SAR data, soil moisture, and surface roughness. Section 6 presents experiment results and discussion. Finally, the conclusions are presented in Section 7.

## 2. RELATIONSHIP BETWEEN RADAR BACKSCATTERING COEFFICIENT AND SOIL PARAMETERS

The backscattering coefficient of SAR systems is the function of the physical and electrical properties of a target and SAR configuration (frequency, incidence angle, and polarization). The backscattering coefficient is influenced by the following factors: (1) the surface roughness. The surface roughness results in the presence of coherent and incoherent parts in the reflection, affecting the overall reflection coefficient; (2) soil moisture affects the permittivity of the surface, and then the backscattering coefficient through the permittivity; (3) SAR satellite signal incidence angle is also an important factor. In microwave radar, incidence angles determine the direction of microwave propagation and the signal intensity received by the antenna. Therefore, the backscattering coefficients of different incidence angles are also different.

To describe the relationship between these parameters, several researchers have proposed empirical models and electromagnetic scattering models (IEM [10], KA [23], and SPM [24]). Based on these models and radar data, Dubois et al. [9] proposed a semi-empirical model to simulate the radar backscattering coefficient in vertical polarization ( $\sigma_{VV}^0$ ) for bare soil surfaces. The expression of  $\sigma_{VV}^0$  depends on the radar wave incidence angle ( $\theta$ ), the real part of the soil dielectric constant ( $\epsilon$ ), the surface roughness ( $RMSH$ ), and the radar wavelength ( $\lambda$ ):

$$\sigma_{VV}^0 = 10^{-2.35} \left( \frac{\cos^3 \theta}{\sin^3 \theta} \right) 10^{0.046\epsilon \tan \theta} (k \cdot RMSH \sin \theta)^{1.1} \lambda^{0.7} \quad (1)$$

where  $k$  is the radar wave number given by  $k = 2\pi/\lambda$ .  $\sigma_{VV}^0$  is given in a linear scale.  $\lambda$  is in cm.  $\varepsilon$  is the soil dielectric constant. The relationship between soil dielectric constant and soil moisture can be described by the Hallikainen model [25]:

$$\varepsilon = (1.993 + 0.002S + 0.015C) + (38.086 - 0.176S + 0.633C) Mv + (10.72 + 1.256S + 1.522C) Mv^2 \quad (2)$$

where  $S$  and  $C$  are the proportions of sand and clay in the soil texture, respectively. The validity of the Dubois model is limited as follows:  $k \cdot RMSH \leq 2.5$ ,  $Mv \leq 35$  vol.%, and  $\theta \geq 30^\circ$ . The parameters of this model are all fixed. Although it illustrates the interrelationships between several variables, it is poorly adapted to different terrains.

To better demonstrate the relationship between radar backscatter coefficient and various parameters in the Dubois model, namely incidence angle, roughness, and soil moisture, the influence of each variable on the backscattering coefficient is simulated by control variates, as shown in Figure 1. Figure 1(a) shows the influence of soil moisture and RMSH to backscattering coefficient. As shown in the figure, when RMSH is constant,  $\sigma_{VV}^0$  increases with the increase of soil moisture. And when soil moisture remains unchanged,  $\sigma_{VV}^0$  increases with the increase of roughness. Figure 1(b) presents the relationship of backscattering coefficient and incidence angle. As the incidence increases,  $\sigma_{VV}^0$  has downward trends, and the decrease is higher for low angles than for high angles when soil moisture and roughness are constant.

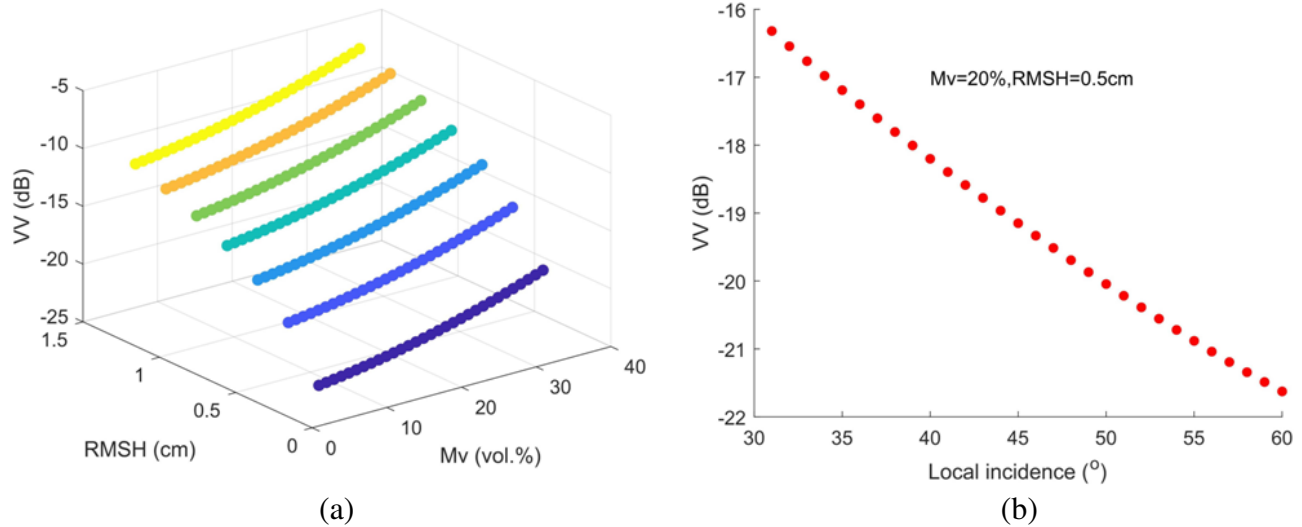


**Figure 1.** Dubois model simulation results for  $VV$  polarization, (a) the effects of  $RMSH$  and  $Mv$  on backscattering coefficient; (b) the relationship between backscattering coefficient and incidence angle.

### 3. EMPIRICAL MODELS FOR RETRIEVING SOIL MOISTURE

#### 3.1. Modified Dubois Model

Through the analysis of various variables in the Dubois model, for bare soil surface, the backscattering coefficient mainly depends on soil roughness ( $RMSH$ ), soil moisture ( $Mv$ ), and SAR sensors' parameters including local incidence angle ( $\theta$ ) and wavelength ( $\lambda$ ). Baghdadi et al. [15] proposed a new modified Dubois model, based on the basis of several bands of radar backscattering coefficient being collected. The model uses the dependency observed between the SAR signal and soil parameters according to results from various studies. Several parameters that can be regulated are also given, such as  $\delta$  and  $\beta$ . In the following section, we use this model to solve specific parameters for the study area. The radar polarization ( $p$  and  $q = H$  or  $V$ , with  $HV = VH$ ) can be expressed as the product of these parameters, as shown in Equation (3):

$$\sigma_{pq}^0 = f_{pq}(\theta) g_{pq}(Mv, \theta) \Gamma_{pq}(k \cdot RMSH, \theta) \quad (3)$$

The first term  $f_{pq}(\theta)$  can be presented as  $f_{pq}(\theta) = \delta(\cos \theta)^\beta$  [26, 27], which illustrates the relation that  $\sigma_{pq}^0$  decreases with the increase of incidence angle.

The second term describes the relation between radar backscattering coefficient and soil moisture ( $Mv$ ). Several studies discovered a linear increase in the relationship between soil moisture and backscattering coefficient, and also in order to show the influence of angle on radar signal,  $g_{pq}(Mv, \theta)$  can be written as  $10^{\gamma \cot(\theta) Mv}$ .

The last term  $\Gamma_{pq}(k \cdot RMSH, \theta)$  shows the relation between radar signal and soil roughness. According to several literatures, the effect of roughness on radar signal is often expressed by logarithmic function [28]. Moreover, incidence angles also affect the sensitivity of radar signal to roughness. Therefore, to integrate the incidence angle and roughness, this term can be written as  $(k \cdot RMSH)^{\xi \sin(\theta)}$ .

As a result, the relationship between the radar backscattering coefficient and soil parameters (soil moisture and surface roughness) for bare soil surface can be written as Equation (4):

$$\sigma_{pq}^0 = \delta (\cos \theta)^\beta 10^{\gamma \cot(\theta) Mv} (k \cdot RMSH)^{\xi \sin(\theta)} \quad (4)$$

where  $\sigma_{pq}^0$  is given in liner scale, and  $\theta$  is expressed in radians.  $Mv$  is in vol.%, and  $k$  is the wave number given by  $k = 2\pi/\lambda$ .  $RMSH$  and  $\lambda$  are both in cm. The coefficients  $\delta$ ,  $\beta$ ,  $\gamma$ , and  $\xi$  are estimated for each radar polarization using the method of least squares based on field data:

$$\sigma_{pq}^0 = \begin{bmatrix} \sigma_{pq,1}^0 \\ \sigma_{pq,2}^0 \\ \sigma_{pq,3}^0 \\ \vdots \\ \sigma_{pq,n}^0 \end{bmatrix}, \quad \theta = \begin{bmatrix} \theta_1 \\ \theta_2 \\ \theta_3 \\ \vdots \\ \theta_n \end{bmatrix}, \quad \mathbf{RMSE} = \begin{bmatrix} RMSE_1 \\ RMSE_2 \\ RMSE_3 \\ \vdots \\ RMSE_n \end{bmatrix}, \quad \mathbf{Mv} = \begin{bmatrix} Mv_1 \\ Mv_2 \\ Mv_3 \\ \vdots \\ Mv_n \end{bmatrix} \quad (5)$$

$$\min(D) = \sum \left( \sigma_{pq}^0 - \delta (\cos \theta)^\beta 10^{\gamma \cot(\theta) Mv} (k \cdot \mathbf{RMSH})^{\xi \sin(\theta)} \right) \quad (6)$$

where  $\sigma_{pq}^0$ ,  $\theta$ ,  $\mathbf{RMSE}$ , and  $\mathbf{Mv}$  are all measured datasets. When  $D$  in Equation (6) is minimized, a set of values is obtained.

In order to estimate soil moisture using modified Dubois model, the inverse solution of Dubois model should be implemented. In the inverse solution of the model, soil moisture is obtained for the relevant polarization as presented in Equation (7).

$$Mv = \frac{\log_{10} \left( \frac{\sigma_{pq}^0}{\delta (\cos \theta)^\beta (k \cdot RMSH)^{\xi \sin(\theta)}} \right)}{\gamma \cot(\theta)} \quad (7)$$

### 3.2. MLR Analysis for Soil Moisture

The other method is to establish a multiple linear relationship after the logarithm of Equation (1). In the estimation for soil moisture, empirical models present correlation among different variables such as  $\theta$ ,  $RMSH$ , and  $\sigma_{pq}^0$  by the approach of regression analysis. Since the mentioned variables mainly affect the process of retrieving soil moisture, Sekertekin et al. [16] considered these variables in empirical model development using MLR analysis:

$$Mv = f(\sigma_{pq}^0, \theta, RMSH) \quad (8)$$

As a result of MLR analysis, the developed model is expressed by Equation (9):

$$Mv = a \cdot \sigma_{pq}^0 + b \cdot \theta + c \cdot RMSH + d \quad (9)$$

where  $\sigma_{pq}^0$  is the backscattering coefficient in dB ( $p$  and  $q$  are  $H$  or  $V$ , with  $HV = VH$ ),  $\theta$  the local incidence angle, and  $RMSH$  the soil roughness. In MLR,  $a$ ,  $b$ ,  $c$ , and  $d$  refer to model coefficients, estimated by the method of least squares based on field data. The model is also flexible, with four parameters determined by field data.

## 4. PROPOSED INVERSE MODELING OF SOIL MOISTURE USING A NEURAL NETWORK

### 4.1. Neural Network Retrieval Approach

One effective method for retrieving soil moisture is to use a neural network, which is also used in this study. Neural networks have strong nonlinear fitting ability, which can map the arbitrarily complex nonlinear relationship between soil parameters and radar backscattering coefficients. The ability is unavailable in empirical models.

In this study, the feed-forward multilayer perceptron neural network available in the Matlab Neural Networks toolbox was considered. This neural network training was based on the back propagation learning rule. The scheme of this implementation followed the strategy presented in [29].

### 4.2. Neural Network Architecture Definition and Training

Figure 2(a) shows the basic structure of the neural network. The structure of the neural networks is such that its input is a three-dimensional vector, and the output is a single-dimensional vector. For this purpose, the input vector contains  $\sigma_{pq}^0$ ,  $\theta$ , and  $RMSH$  values, and the output contains the soil moisture.  $\sigma_{VV}^0$ ,  $\theta$  and  $RMSH$  are used as inputs in Section 6.3.1, and  $\sigma_{VV}^0$ ,  $\sigma_{VH}^0$ ,  $\theta$ , and  $RMSH$  are used in Section 6.3.2.

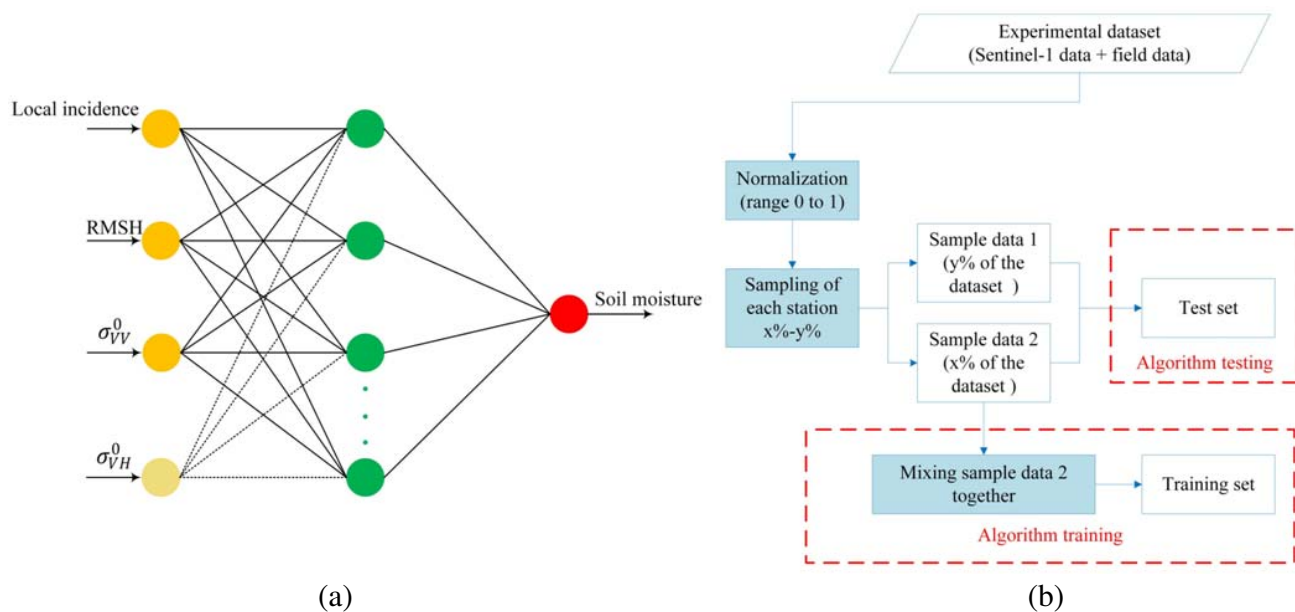


**Figure 2.** (a) Example of neural network scheme, (b) work flow of the generation of training and test dataset.

In the neural network, a hidden layer is considered as a layer between the input and output layers. In this layer, neurons are applied as weighted inputs, and an activation function is used to create an output or a series of outputs. The neural network used in this study included 20 neurons in the hidden layer.

A flowchart of the generation of training and test datasets is shown in Figure 2(b). The data considered for training and testing the algorithm are derived from Sentinel-1A SAR images, combined with the corresponding field data, which is described in the following section. The main reason to use field data instead of simulated data is providing rather reliable data by which the neural network can be well trained for predicting soil moisture. Because the in-situ data vary greatly, they need to be unified into a range. Data preprocessing is necessary before neural network training. The data preprocessing is divided into the following three steps:

- (1) The data are normalized to ensure that the data at each site are within a range of 0 to 1, thus eliminating the adverse effects caused by the singular sample data.
- (2) 75% of sample points are selected from each site as sample data 2, and the remaining data are used for sample data 1. When selecting the data, the radar backscatter coefficient in the data is guaranteed to be highly sensitive to the change of soil moisture.
- (3) The sample data 1 from each site are mixed as training set and input into the network to train the network. The trained network is utilized to test each site's data.

## 5. DATASETS

For a better understanding of the performance for each inversion method, field data are collected. In addition, the radar backscatter coefficient needs to be extracted from Sentinel-1A. This section mainly focuses on the field data and SAR data collection.

### 5.1. Study Area and Spaceborne SAR Data

An agricultural region in Baoxie in Wuhan, which is a district of Hubei Province in China, was selected as the study area, as shown in Figure 3. Figure 3 presents a map of Baoxie from Google earth, and the SAR image from Sentinel-1. The terrain of this region is relatively flat, and most of it has similar physiognomy features, with only a small part being different. The soil roughness in this region was almost unchanged during the obtainment of the SAR image. In addition, the vegetation cover is small, which reduces the influence of vegetation on the inversion process and is conducive for reflecting the change in retrieved soil moisture over time, according to field investigation. The soil texture is generally classified as loam (51.51% sand and 13.43% clay).

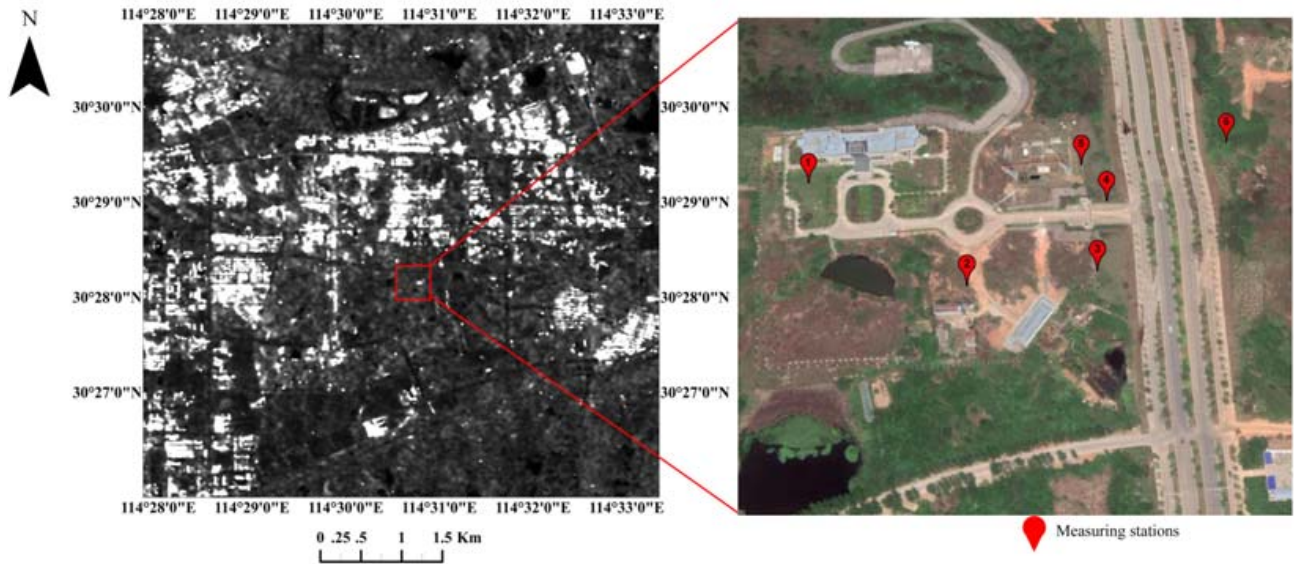


**Figure 3.** Study area and measurement stations distribution.

Sentinel-1 satellites, including Sentinel-1A and Sentinel-1B, are equipped with a C-band SAR instrument that provides data in dual polarizations. Sentinel-1A provides a 12-day repeat cycle and 175 orbits per cycle. Sentinel-1B provides the same repeat cycle and orbits with a  $180^\circ$  orbital phasing difference. Currently, with 1A and 1B operating, the ideal cycle in most regions is six days. The SAR images used in this study were mainly provided by Sentinel-1A.

Sentinel-1 mission provides open-access data to users, and all data can be freely downloaded through the Copernicus Open Access Hub. The images are acquired in IW (wide swath) mode at VV and VH

polarizations. Additionally, all images are in an ascending pass (track 113) with a mean incidence angle of  $44^\circ$ . The level-1 ground range detected (GRD) product and single look complex (SLC) product were used in this study. SLC images are converted to GRD images in SNAP software to extract parameters. Sentinel-1A data of 12 days from November 2019 to April 2020 are selected for subsequent experiments.

## 5.2. Field Data and Sensitivity Analysis of SAR Data to In-Situ Moisture

In this research, soil moisture and roughness are conjointly measured the same day as the SAR data acquisitions. Soil surface moisture ( $Mv$  in vol.%) was measured in six different measurement sites. The in-situ data were obtained from November 2019 to April 2020. Soil moisture measurements at these sites were performed at a depth of 5 cm and with 1 h time interval. As illustrated in Figure 4(a), the measuring equipment used a probe to measure soil moisture.

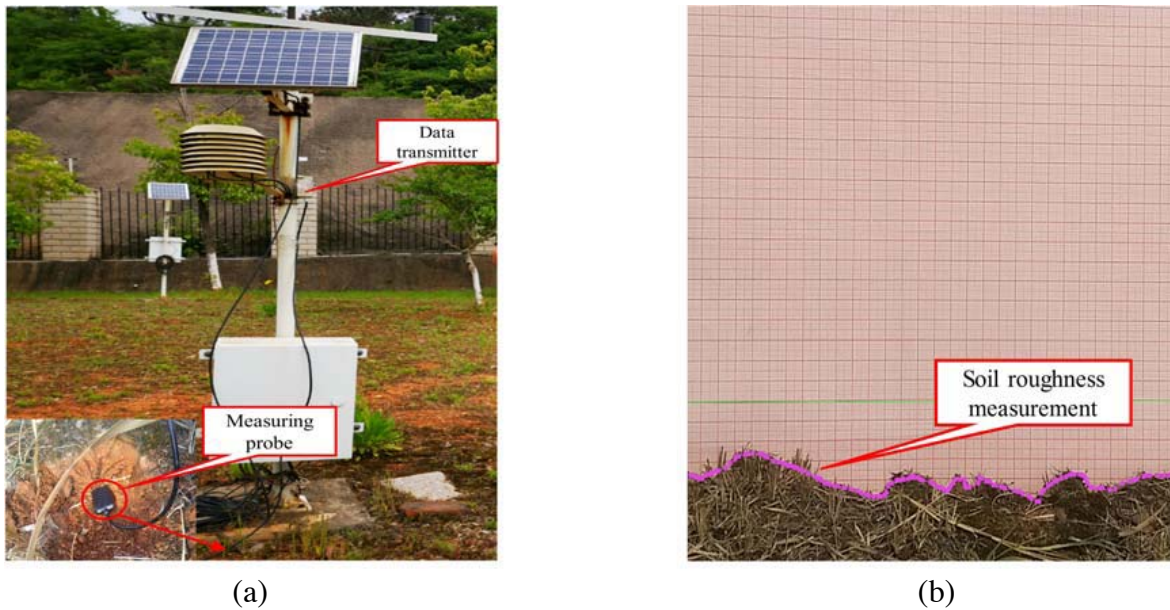


**Figure 4.** (a) Soil moisture measuring device. (b) A roughness device made in the laboratory.

The roughness ( $RMSH$ ) was also measured with a home-made profilometer and a digital camera, as shown in Figure 4(b). In order to provide accurate surface roughness results, four profiles were recorded for each test site. On average, two parallel and two perpendicular measurements are made for each land site. After the measurement, the soil profile was drawn through discrete points on the red coordinate paper, and the  $X$ - $Y$  axis was established on the scale of the coordinate paper. The coordinates of the points depicted were recorded, and  $RMSH$  was calculated based on Equation (10). Since four measurements were collected from each site, the mean of measurements was utilized for further analysis in each test station.

$$RMSH = \sqrt{\frac{\sum_{i=1}^N (Z_i - \bar{Z})^2}{N - 1}} \quad (10)$$

where  $N$  is the number of profile points,  $Z_i$  the surface elevation at point  $i$  in cm, and  $\bar{Z}$  the average.

In this study, since the  $VV$  polarization backscattering coefficient has the same effect on estimating soil moisture as the  $VH$  polarization, we use the  $VV$  polarization as a data source to compare the abilities of different methods for estimating. The sensitivity of the SAR signal to soil moisture in  $VV$  polarization is analyzed for six different measuring stations. As shown in Table 1, the  $R^2$  difference in

**Table 1.**  $R^2$  of the  $\sigma_{VV}^0$  to in-situ moisture for each station.

	Station 1	Station 2	Station 3	Station 4	Station 5	Station 6
$R^2$	0.1562	0.233	0.0682	0.3238	0.6243	0.1754

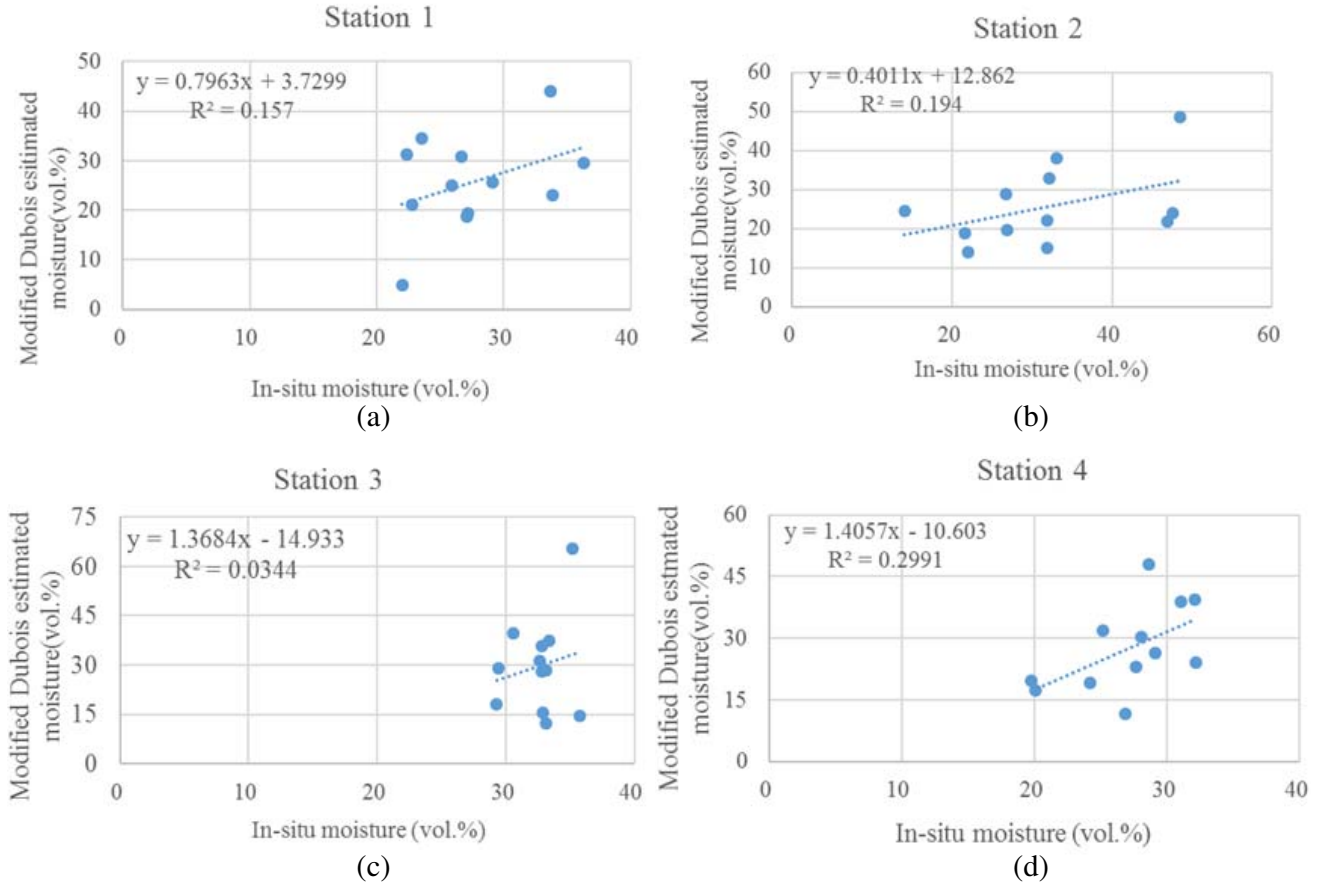
measuring stations is relatively large from 0.0682 to 0.6243, but the correlation between soil moisture and backscattering coefficient meets the experiment requirement on the whole.

As shown in Table 1,  $R^2$  between in-situ moisture and  $\sigma_{VV}^0$  of stations 1, 3, and 6 is lower than that of the other three sites. There are two reasons for this difference. The first reason is the fluctuation error of the moisture sensor. Due to the use of electronic sensors, zero wander exists inside the sensor. The second reason is backscatter data errors. In rainy weather, the backward scattering coefficient decreases due to the occurrence of water accumulation at some measuring stations, which is inconsistent with the trend of soil moisture and reduces the correlation.

## 6. EXPERIMENT RESULTS OF SOIL MOISTURE AND DISCUSSION

### 6.1. Performance of Modified Dubois Model

To evaluate the performance of the modified Dubois model for estimating soil moisture, 75% of the datasets for each measurement station were utilized for training the data, and 25% of datasets were used for testing purposes. Figure 5 shows the training and testing results based on the modified Dubois model. As illustrated in Figures 5(d), 5(e), and 5(f), the estimated soil moisture in stations 4, 5, and 6 is highly correlated with the in-situ moisture, with  $R^2$  being 0.2991, 0.6082, and 0.2775, respectively.



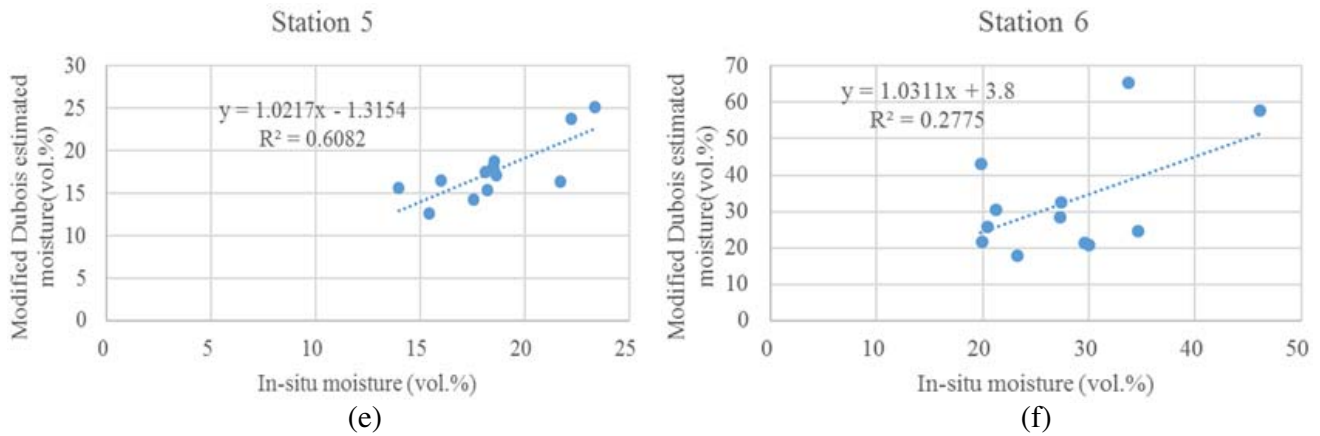


**Figure 5.** The training and testing results of the modified Dubois model (a) station 1; (b) station 2; (c) station 3; (d) station 4; (e) station 5; (f) station 6.

**Table 2.** RMSE results of the modified Dubois model for each station.

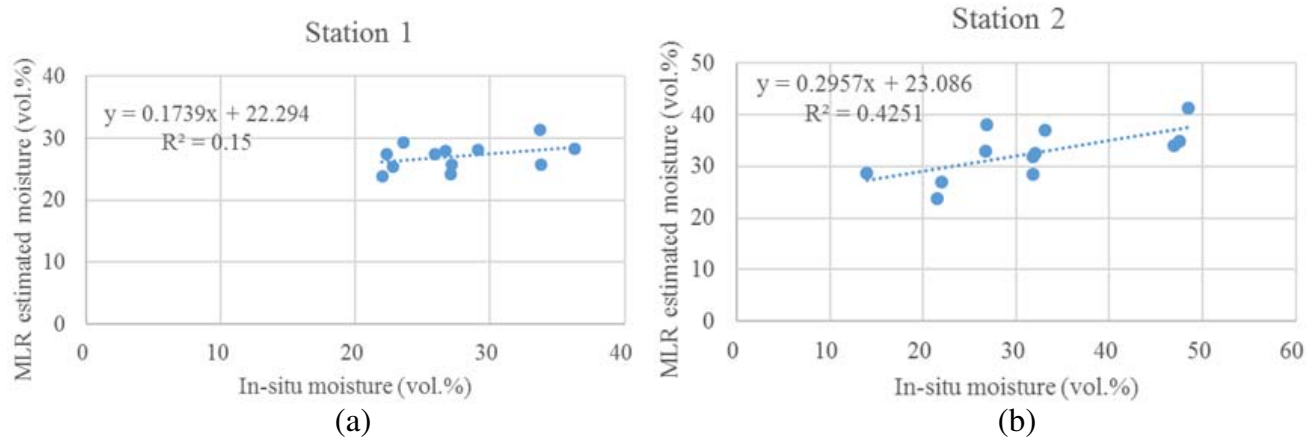
	Station 1	Station 2	Station 3	Station 4	Station 5	Station 6
RMSE (vol.%)	7.55	10.76	10.33	7.88	3.30	12.08

Figures 5(a) and 5(b) show that  $R^2$  of stations 1 and 2 are 0.157 and 0.194, respectively. As indicated in Figure 5(c), station 3 has a low correlation coefficient with  $R^2$  being 0.0344. Table 2 shows the results of RMSE for each station. As shown in table, stations 1, 4, and 5 have lower RMSE (7.55 vol.%, 7.88 vol.% and 3.30 vol.%, respectively), indicating that the estimated moisture of the two sites are more similar to the in-situ data values. The remaining stations all have RMSE values greater than 10 vol.%.

Overall, the correlation between estimated moisture and in-situ moisture is consistent with the correlation trend between SAR signals and in-situ data, with stations 4 and 5 having the best results from both RMSE and  $R^2$ .

### 6.2. Performance of MLR Analysis

In order to ensure the reliability of MLR analysis, the selection of training data and test data should be consistent with the test process of the modified Dubois model. Figure 6 shows the training and testing results of the MLR analysis. As presented in Figures 6(b), 6(d), and 6(e), stations 2, 4, and 5 have high



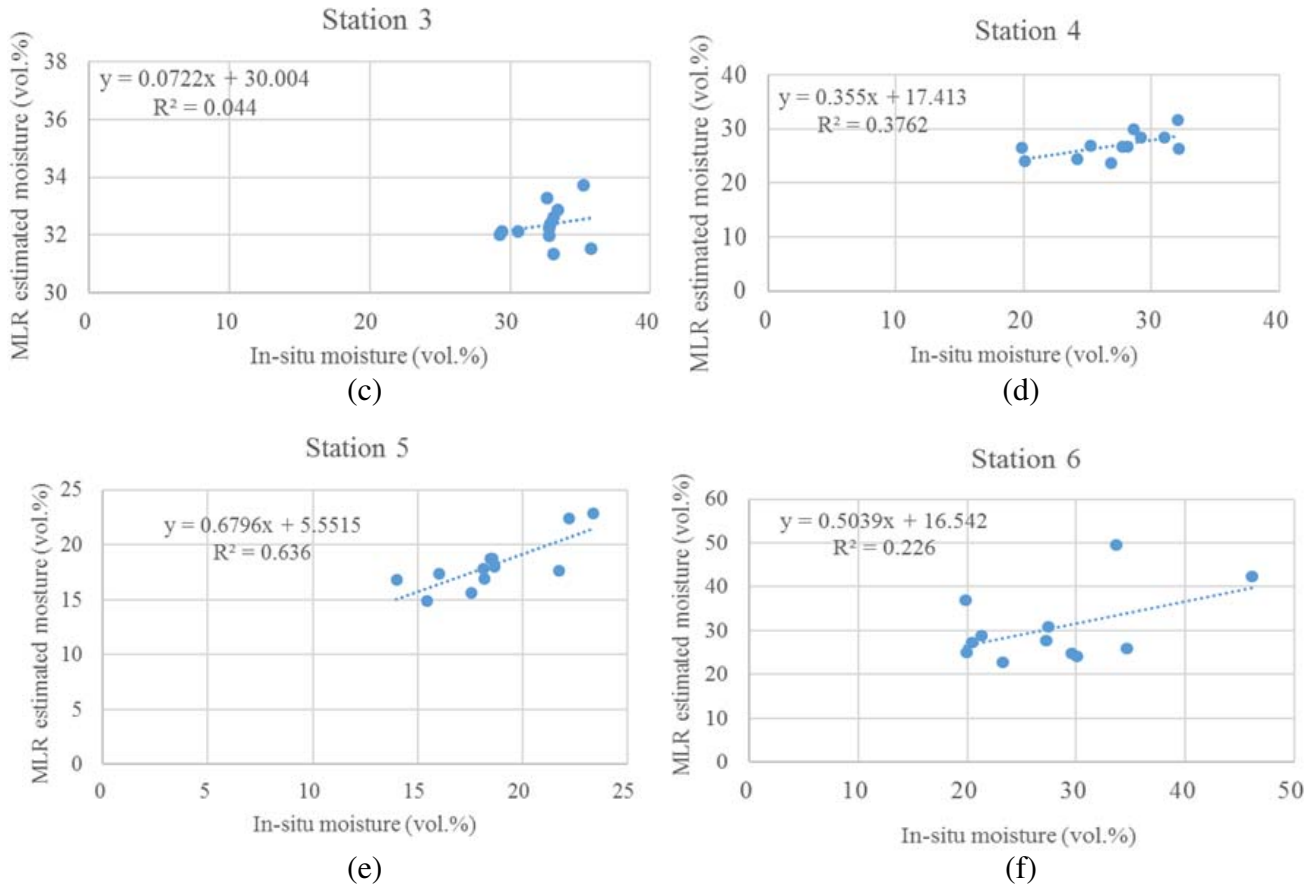


**Figure 6.** The training and testing results of the MLR analysis (a) station 1; (b) station 2; (c) station 3; (d) station 4; (e) station 5; (f) station 6.

**Table 3.** RMSE results of the MLR analysis for each station.

	Station 1	Station 2	Station 3	Station 4	Station 5	Station 6
RMSE (vol.%)	3.66	8.33	1.45	3.20	2.53	7.97

correlation between estimated moisture and in-situ moisture, with  $R^2$  being 0.4251, 0.3762, and 0.636, respectively. Station 3 still has a low correlation coefficient, with  $R^2$  being only 0.044. Table 3 shows the results of RMSE for each station. The table displays that the RMSEs of six stations are from 1.45 vol.% to 7.97 vol.% for MLR analysis.

Compared with the modified Dubois model,  $R^2$  of stations 2, 4, and 5 are increased by 0.2311, 0.0771, and 0.0278, respectively. Also, from the perspective of RMSE, the MLR estimation of soil moisture is more approximate to the in-situ data than the one through the modified Dubois model. In general, the MLR analysis performs better than the Dubois model in both  $R^2$  and RMSE for estimating soil moisture.

### 6.3. Estimation of Soil Moisture Using Neural Networks

After analyzing the training and testing results of soil moisture by the modified Dubois model and MLR analysis, it is necessary to analyze the ability of soil moisture inversion using a neural network and compare it with the other two models. The neural network takes advantage of the possibility

to combine multiple sources of information into the same retrieval algorithm. In order to consider the accuracy and correlation of soil moisture inversion under different input conditions, we first use three parameters ( $\sigma_{VV}^0$ ,  $\theta$  and  $RMSH$ ) as inputs in the following Section 6.3.1 and then consider four parameters ( $\sigma_{VV}^0$ ,  $\theta$  and  $RMSH$  plus  $\sigma_{VH}^0$ ) as inputs in Section 6.3.2.

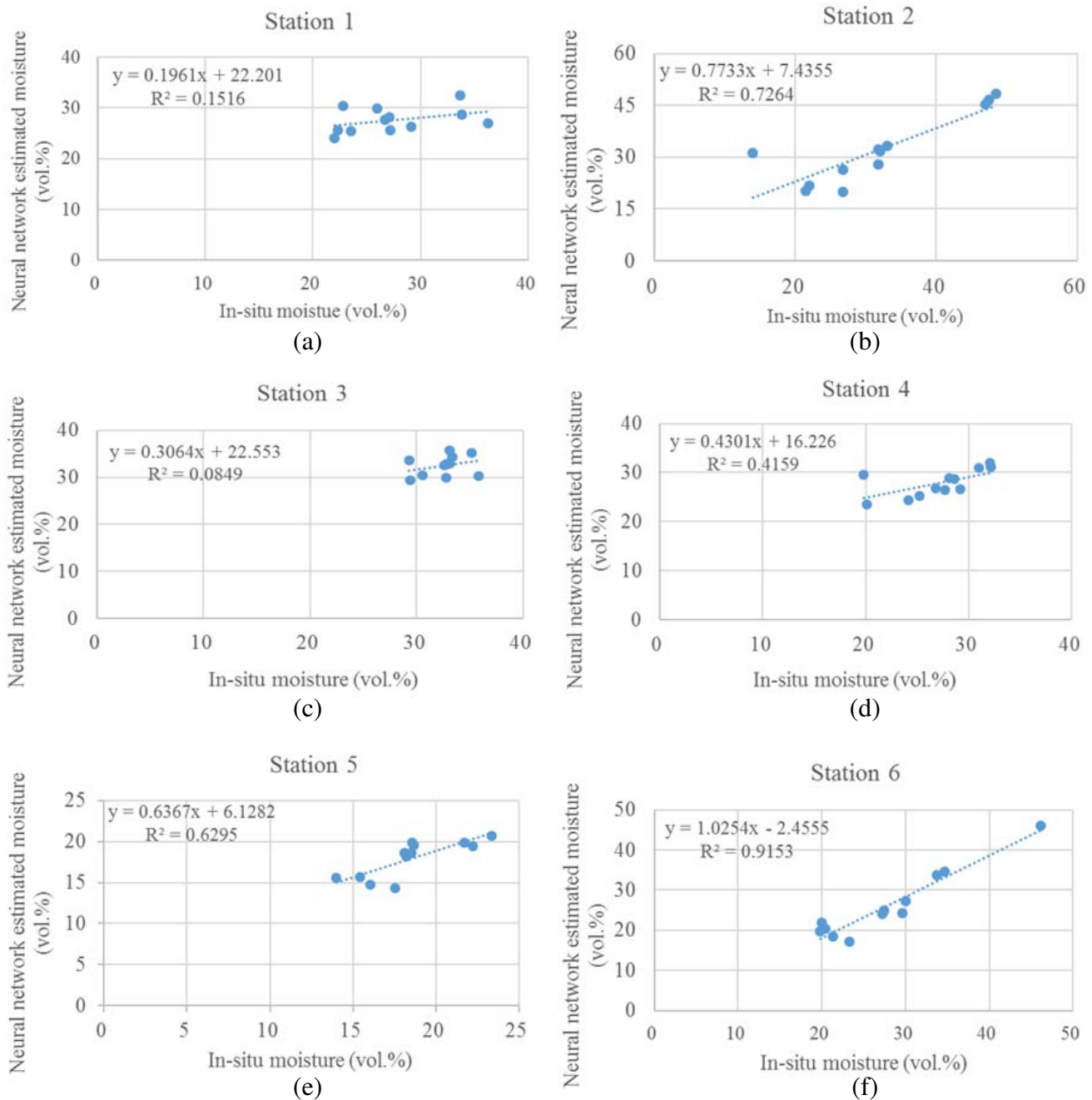


**Figure 7.** The training and testing results of the estimation using neural network (a) station 1; (b) station 2; (c) station 3; (d) station 4; (e) station 5; (f) station 6.

6.3.1.  $\sigma_{VV}^0$ ,  $\theta$ , and RMSH as Inputs

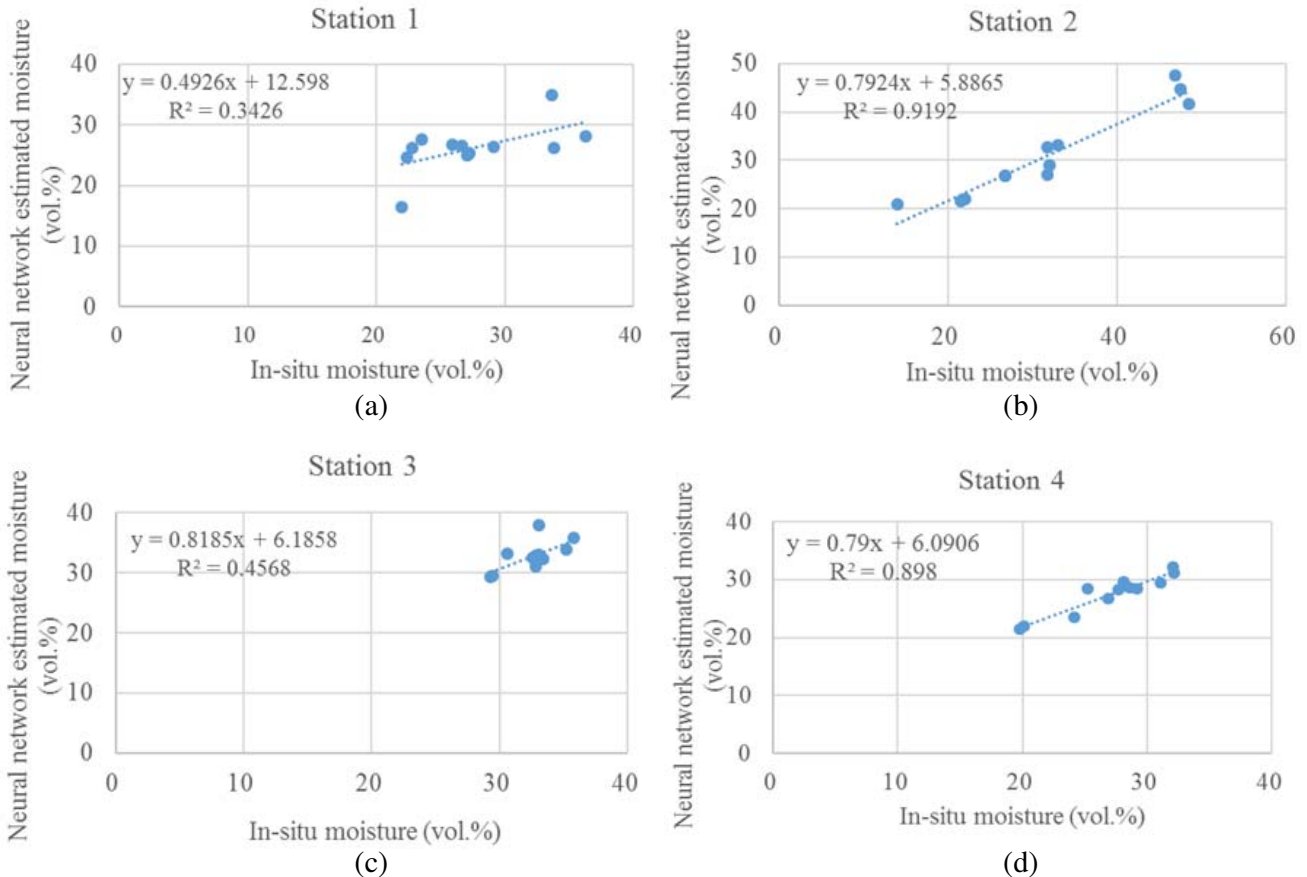
The soil moisture is estimated based on the neural network architecture provided in previous Section 4.2. Figure 7 shows the training and testing results of the estimation for each station. Compared with the results of the modified Dubois model and MLR analysis, Figure 7 illustrates that the neural network has an improvement in  $R^2$  on estimating soil moisture. Figures 7(b), 7(d), 7(d), and 7(f) show that the estimated soil moisture of stations 2, 4, 5, and 6 has high correlation with in-situ moisture, with  $R^2$  being 0.7264, 0.4159, 0.6295, and 0.9153. Compared with the MLR analysis,  $R^2$  of stations 2, 4, and 6 are improved by 0.3013, 0.0397, and 0.6893, respectively. As indicated in Figures 7(a) and 7(c), a slight improvement over MLR analysis is also noticed, with  $R^2$  increasing by 0.0016 and 0.0409, respectively.

Table 4 shows RMSE results of the estimation for each station. As shown in the table, the RMSE is from 2.68 vol.% to 10.81 vol.%. Compared with the modified Dubois model, this method has a great improvement in RMSE, which is similar to the RMSE of MLR analysis, and can well estimate the measured soil moisture.

**Table 4.** RMSE results of the estimation using neural network for each station.

	Station 1	Station 2	Station 3	Station 4	Station 5	Station 6
RMSE (vol.%)	3.74	10.24	1.99	3.45	2.48	7.95

To sum up, the inversion effect of soil moisture using a neural network is better than the other two methods.



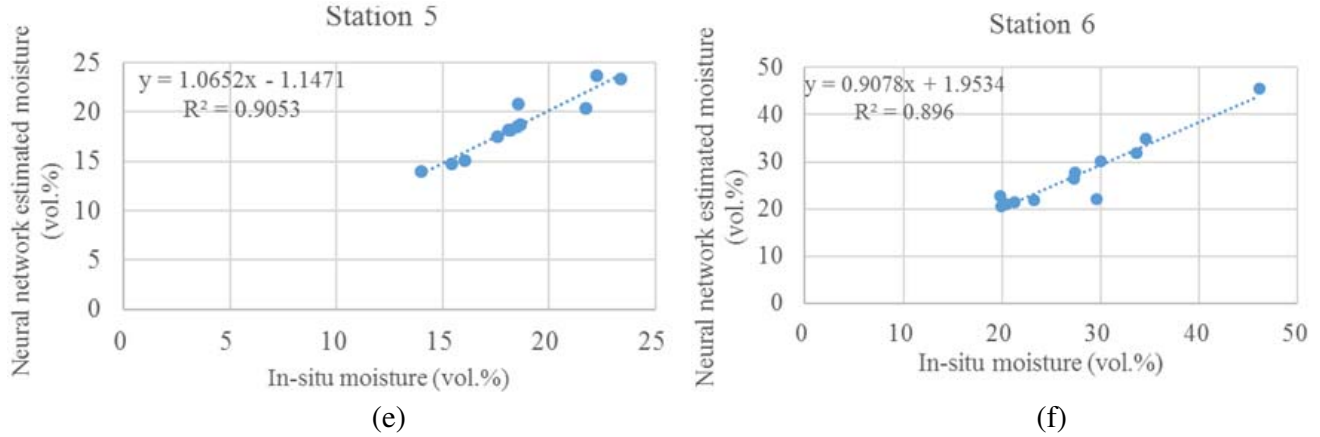


**Figure 8.** The training and testing results of the estimation using neural network based on  $VV$  and  $VH$  polarizations (a) station 1; (b) station 2; (c) station 3; (d) station 4; (e) station 5; (f) station 6.

**Table 5.** RMSE results of the estimation using neural network for each station based on  $VV$  and  $VH$  polarizations.

	Station 1	Station 2	Station 3	Station 4	Station 5	Station 6
RMSE (vol.%)	4.41	9.85	2.16	3.72	2.88	7.47

6.3.2.  $\sigma_{VV}^0, \sigma_{VH}^0, \theta$ , and  $RMSH$  as Inputs

In order to study the influence of multi-polarization data on the correlation and accuracy of inversion results, we took  $\sigma_{VV}^0, \sigma_{VH}^0, \theta$ , and  $RMSH$  as input parameters and put them into the neural network for training, and acquired better inversion results than single polarization backscattering coefficient as input. Figure 8 shows the training and testing results of the estimation based on  $\sigma_{VH}^0$  and  $\sigma_{VV}^0$  polarizations. As shown in Figures 8(b), 8(d), 8(e), and 8(f),  $R^2$  of stations 2, 4, 5, and 6 all reached about 0.9, which have increased compared with the input condition in Section 6.3.2. Moreover, as shown in Figure 8(c),  $R^2$  of station 3 has also been improved significantly by 0.3719, compared with single polarization. Table 5 shows the RMSE of the estimated results. As can be seen from the table, there is not much change in the estimation accuracy, compared to using only  $\sigma_{VV}^0$  as the input.

In general, with  $\sigma_{VV}^0, \sigma_{VH}^0, \theta$ , and  $RMSH$  as inputs, the inversion soil moisture of the neural network shows an increase in correlation coefficient. In other words, when multiple parameters related to soil moisture are used for inputs in neural network, the inversion results are productive.

7. CONCLUSIONS

The major objective of this study is to evaluate the capability of bare soil moisture estimation for a neural network and two empirical models, namely modified Dubois model and MLR analysis, based on Sentinel-1 images. To ensure the reliability and accuracy of the experiment, we collected SAR data for 12 days and real-time soil data (roughness and moisture) from 6 measurement sites.

By analyzing the relationship between estimated soil moisture at each station and in-situ data, the results of stations 2, 4, and 5 indicate that the correlation of estimated soil moisture by the MLR analysis improves by 0.2311, 0.0771, and 0.0278, respectively, compared with the modified Dubois model. And RMSE of the modified Dubois model is on average 4.12 vol.% higher than that of MLR analysis, meaning that MLR estimation is more approximate in in-situ data. Moreover in comparison with MLR analysis, better experimental results are obtained in stations 2, 4, and 5 with the neural network, with  $R^2$  being improved by 0.3013, 0.0397, and 0.6893, respectively. The RMSE of inversion results by the neural network is similar to that of the MLR analysis.

Apart from analyzing the ability of three methods to retrieve soil moisture, we also discussed the ability of neural network to retrieve soil moisture under different input conditions. The results show that when  $\sigma_{VV}^0$ ,  $\sigma_{VH}^0$ ,  $\theta$ , and  $RMSH$  are jointly input into the neural network, the correlation of the inversion results increases, and  $R^2$  of stations 2, 4, 5, and 6 reach about 0.9, which illustrates that the trend of estimated soil moisture is similar to in-situ moisture.

One of the limitations of this study is that the data of stations 1, 3, and 6 that we collected have low correlation coefficient due to the errors of sensor. However, it would be better if the data of each station can be calibrated. Thus, the performance evaluation might give better results. In addition to this limitation, further researches are required to obtain better results in estimating soil moisture with SAR data, and we even believe that the results of this study will shed light on future studies. Future studies can be given as follows:

- (1) The longitude and latitude of each measurement station can be considered into the neural network. Through the training of coordinates, the range of soil moisture in different areas can be divided.
- (2) Considering the vegetation cover coefficient, the neural network inversion model can be extended to the vegetation removal area.

## ACKNOWLEDGMENT

This paper is supported by the National Key R&D Program of China under grant 2018YFB2100500.

## REFERENCES

1. Pacheco, A., et al., "The impact of national land cover and soils data on SMOS soil moisture retrieval over Canadian agricultural landscapes," *IEEE Journal of Selected Topics in Applied Earth Observations and Remote Sensing*, Vol. 8, No. 11, 5281–5293, 2015.
2. Zhu, G., et al., "Relative soil moisture in China's farmland," *Journal of Geographical Sciences*, Vol. 29, 334–350, 2019.
3. Azimi, S., et al., "Understanding the benefit of Sentinel 1 and SMAP-era satellite soil moisture retrievals for flood forecasting in small basins: Effect of revisit time and the spatial resolution," *Journal of Hydrology*, Vol. 581, 2019.
4. Ma, S.-C., et al., "Effects of controlling soil moisture regime based on root-sourced signal characteristics on yield formation and water use efficiency of winter wheat," *Agricultural Water Management*, Vol. 221, 486–492, 2019.
5. Dari, J., et al., "Spatial-temporal variability of soil moisture: Addressing the monitoring at the catchment scale," *Journal of Hydrology*, Vol. 570, 2019.
6. Gao, Q., et al., "Synergetic use of Sentinel-1 and Sentinel-2 data for soil moisture mapping at 100 m resolution," *Sensors*, Vol. 17, 1966, 2017.
7. Paloscia, S., et al., "Soil moisture mapping using Sentinel-1 images: Algorithm and preliminary validation," *Remote Sensing of Environment*, Vol. 134, 234, 2013.
8. Ulaby, F., et al., *Microwave Radar and Radiometric Remote Sensing*, Artech House, 2014.
9. Dubois, P. C., J. V. Zyl, and T. Engman, "Measuring soil moisture with imaging radars," *IEEE Transactions on Geoscience and Remote Sensing*, Vol. 33, No. 4, 915–926, 1995.
10. Fung, A. K., *Microwave Scattering and Emission Models and Their Applications*, Artech House, Norwood, MA, 1994.
11. Oh, Y., K. Sarabandi, and F. Ulaby, "Semi-empirical model of the ensemble-averaged differential Mueller matrix for microwave backscattering from bare soil surfaces," *IEEE Transactions on Geoscience and Remote Sensing*, Vol. 40, 1348–1355, 2002.
12. Oh, Y., K. Sarabandi, and F. T. Ulaby, "An empirical-model and an inversion technique for radar scattering from bare soil surfaces," *IEEE Transactions on Geoscience and Remote Sensing*, Vol. 30, 370–381, 1992.

13. Kumar, A., et al., "Study of empirical approaches for retrieval of soil moisture in Solani river catchment area of Uttarakand, India," *2016 11th International Conference on Industrial and Information Systems (ICIIS)*, 481–485, 2016.
14. Baghdadi, N., et al., "Evaluation of radar backscattering models IEM, Oh, and Dubois for SAR data in X-band over bare soils," *IEEE Geoscience and Remote Sensing Letters*, Vol. 8, 1160–1164, 2011.
15. Baghdadi, N., et al., "A new empirical model for radar scattering from bare soil surfaces," *Remote Sensing*, Vol. 8, 920, 2016.
16. Sekertekin, A., A. Marangoz, and S. Abdikan, "ALOS-2 and Sentinel-1 SAR data sensitivity analysis to surface soil moisture over bare and vegetated agricultural fields," *Computers and Electronics in Agriculture*, Vol. 171, 1–11, 2020.
17. Santi, E., et al., "Remote sensing of forest biomass using GNSS reflectometry," *IEEE Journal of Selected Topics in Applied Earth Observations and Remote Sensing*, 2020.
18. Yuan, Q., et al., "Estimating surface soil moisture from satellite observations using a generalized regression neural network trained on sparse ground-based measurements in the continental U.S.," *Journal of Hydrology*, Vol. 580, 124351, 2020.
19. Achieng, K. O., "Modelling of soil moisture retention curve using machine learning techniques: Artificial and deep neural networks vs support vector regression models," *Computers & Geosciences*, Vol. 133, 104320, 2019.
20. Mirsoleimani, H., et al., "Bare soil surface moisture retrieval from Sentinel-1 SAR data based on the calibrated IEM and dubois models using neural networks," *Sensors*, Vol. 19, 3209, 2019.
21. Kweon, S. and Y. Oh, "Estimation of soil moisture and surface roughness from single-polarized radar data for bare soil surface and comparison with dual- and quad-polarization cases," *IEEE Transactions on Geoscience and Remote Sensing*, Vol. 52, No. 7, 4056–4064, 2014.
22. Picard, G., T. Le Toan, and F. Mattia, "Understanding C-band radar backscatter from wheat canopy using a multiple-scattering coherent model," *IEEE Transactions on Geoscience and Remote Sensing*, Vol. 41, 1583–1591, 2003.
23. Beckmann, P. and A. Spizzichino, *The Scattering of Electromagnetic Waves From Rough Surfaces*, 511, Artech House, Inc., Norwood, MA, 1987.
24. Engman, E. and N. Chauhan, "Status of microwave soil moisture measurements with remote sensing," *Remote Sensing of Environment*, Vol. 51, 189–198, 1995.
25. Hallikainen, et al., "Microwave dielectric behavior of wet soil — Part 1: Empirical models and experimental observations," *IEEE Transactions on Geoscience and Remote Sensing*, Vol. 23, No. 1, 25–34, 1985.
26. Beauchemin, M., K. Thomson, and G. Edwards, "Modelling forest stands with MIMICS: Implications for calibration," *Canadian Journal of Remote Sensing*, Vol. 21, 518–526, 1995.
27. Baghdadi, N., M. Bernier, and R. Neeson, "Evaluation of C-band SAR data for wetlands mapping," *International Journal of Remote Sensing*, Vol. 22, 71–88, 2001.
28. Baghdadi, N., N. Holah, and M. Zribi, "Soil moisture estimation using multi-incidence and multi-polarization ASAR SAR data," *International Journal of Remote Sensing*, Vol. 27, 2006.
29. Santi, E., et al., "Application of artificial neural networks for the soil moisture retrieval from active and passive microwave spaceborne sensors," *International Journal of Applied Earth Observation and Geoinformation*, Vol. 48, 2015.